

Self-organizing Energy Management Modeling for Multi-microgrids in Contingencies

Jiachen Chen, *Student Member, IEEE*, Zhong Chen, *Member, IEEE*, and Qiang Xing, *Member, IEEE*

Abstract—Contingencies, such as behavior shifts of microgrid operators (MGOs) and abrupt weather fluctuations, significantly impact the economic operations of multi-microgrids (MMGs). To address these contingencies and enhance the economic and autonomous performance of MGOs, a self-organizing energy management modeling approach is proposed. A second-order stochastic dynamical equation (SDE) is developed to accurately characterize the self-organizing evolution of the operating cost of MGO incurred by contingencies. Firstly, an operating model of MMG relying on two random graph-driven information matrices is constructed and the order parameters are introduced to extract the probabilistic properties of variations in operating cost. Subsequently, these order parameters, which assist individuals in effectively capturing system correlations and updating state information, are incorporated as inputs into second-order SDE. The second-order SDE is then solved by using the finite difference method (FDM) within a loop-structured solution framework. Case studies conducted within a practical area in China validate that the proposed self-organizing energy management model (SEMM) demonstrates spontaneous improvements in economic performance compared with conventional models.

Index Terms—Contingency, energy management, multi-microgrid (MMG), graph, stochastic dynamic equation (SDE), self-organizing feature.

I. INTRODUCTION

MICROGRID (MG) is widely recognized for its efficient utilization of renewable energy sources (RESs) [1]. Multi-microgrid (MMG) systems associate different microgrid operators (MGOs) as an integrated entity that actively engages in economic operations [2]. However, the integration introduces the risk of economic losses due to abrupt changes in RES generation and decision-making of MGOs [3], [4]. To effectively mitigate the impact of these contingencies on economic performance, it is imperative to establish an autonomous and resilient energy management model.

Manuscript received: January 2, 2024; revised: May 24, 2024; accepted: July 26, 2024. Date of CrossCheck: July 26, 2024. Date of online publication: August 26, 2024.

This work was supported by the National Natural Science Foundation of China (No. 52077035) and the Liaoning Revitalization Talents Program of China (No. XLYC2007181).

This article is distributed under the terms of the Creative Commons Attribution 4.0 International License (<http://creativecommons.org/licenses/by/4.0/>).

J. Chen and Z. Chen (corresponding author) are with the School of Electrical Engineering, Southeast University, Nanjing, China (e-mail: 230228741@seu.edu.cn; chenzhong_seu@163.com).

Q. Xing is with the College of Automation & College of Artificial Intelligence, Nanjing University of Posts and Telecommunications, Nanjing, China (e-mail: xingqiang0828@163.com).

DOI: 10.35833/MPCE.2024.000007

Until now, various studies have focused on the modeling method for MMG systems. An effective energy trading (ET) mechanism is a crucial aspect of MMG energy management modeling [5]–[7]. In [5], a contribution-based ET mechanism among MGs is developed, which allocates surplus energy to consumers based on historical contributions. A non-cooperative game-based method wherein buyers compete with each other for allocation using priority factors is presented in [6]. Additionally, a dynamic energy interaction mechanism based on individual contributions is proposed to address the complex business relationships involving multiple owners [7]. However, these studies are primarily driven by individual interests, which pay limited attention to modeling the dynamic cooperative relationships inherent in MMG systems. In this paper, we propose a novel self-organizing energy management model (SEMM) for MMGs that relies on graph-driven information matrices to store ET information derived from random graphs and extract probabilistic properties on ET among MGOs.

Accurately addressing the uncertainties associated with RES and operator decision-making becomes a significant challenge in energy system modeling. A prominent methodology involves incorporating operational research-based modules into the energy system modeling. The scenario-based random optimization [8], [9] and robust optimization [10] are widely applied. However, the former heavily relies on the quantity and quality of the scenario set, while the latter requires consideration of worst-case scenarios that may never occur, inevitably sacrificing a portion of the economic efficiency. The aforementioned issues are effectively addressed through a series of enhancements [11]–[14]. A novel multi-stage robust scheduling for MGs with energy storage to balance the uncertain load and significantly reduce electricity cost is developed in [11]. In [12] and [13], a distributionally robust (DR) optimization model is presented for the resilient operation of integrated electricity and heat energy distribution and MG systems under uncertainties. A moment-based DR model is proposed for distribution network configuration problems with random contingencies in [14]. However, these above studies provide unsatisfactory performances when faced with relatively sparse historical data such as abrupt changes in operator behaviors.

In addition to the above-mentioned operational research-based models, the data-driven agent model based on Markov decision process (MDP) offers an alternative avenue for addressing uncertainties. Especially, the partially observable

MDP (POMDP) model is introduced in [15]. The POMDP model treats the acquired system state as uncertain, providing the partially observed system state to the agent, which then adapts the probability distribution of historical data to estimate the actual state. This model aligns more closely with practical power system operations. Therefore, it has undergone refinements and is applied in energy management [16], resilience-focused dispatch control [17], and reactive power optimization [18], [19] for MG and distribution systems. Similar to DR model, the MDP model also requires retraining with relevant data when encountering unfamiliar operating scenarios. The dependence on external factors highlights limitations in terms of spontaneous adjustments, ultimately impacting economic operations.

The above-mentioned studies exhibit passivity towards uncertain contingencies and negatively impact the economic performance in the event of data sparsity. Therefore, it is imperative to explore modeling techniques that do not rely solely on data and can autonomously adapt to uncertainties.

Stochastic dynamics is a crucial branch of self-organizing theory [20]-[22]. It formulates the changes in complex systems as state transitions and models the process of individual state transitions with uncertain events as a probability-driven stochastic dynamical equation (SDE), which is a differential equation. Specific differential terms in SDE characterize the state transition caused by uncertainty and the self-organizing process that emerges new states after such transitions. This process eliminates passive data-driven approaches and represents a spontaneous evolutionary phenomenon. Although stochastic dynamics demonstrate significant advantages in election prediction modeling [22], their application in energy management modeling for MMG is still in its infancy. In our previous study [23], a first-order SDE is employed to model the MMG system with small-scale uncertainties. However, it fails to capture the dynamic trends in system state transitions resulting from uncertainties, particularly in the context of strong contingencies in MMG. Therefore, by considering the operating costs of MGO as the state, we propose a novel second-order SDE to accurately describe the trend of the self-organizing evolution of the state, specifically referring to operating costs of MGO in contingencies.

To this end, this study proposes a novel SEMM to accurately characterize the self-organizing evolution of the operating cost of MGOs. The main contributions can be summarized as follows.

1) A random graph-based ET model that incorporates the interrelationships among MGs as node connections within a random graph structure is proposed. Two random graph-driven information matrices are constructed to store ET information and extract the probabilistic properties of variations in the operating cost.

2) A second-order SDE is developed to enhance the economic performance of MGOs in contingencies. We consider the operating cost of MGOs as the state, and mathematically represent the state transition as the second-order SDE based on order parameters. These parameters precisely depict the state transition as a self-organizing evolution process in con-

tingencies. The second-order SDE effectively rectifies the unforeseen impact on state transitions, particularly in scenarios lacking historical data.

3) We further verify the practicability of the proposed SEMM by applying it to a realistic MMG system. Simulation results demonstrate its spontaneity and superiority in improving the economic performance when facing abrupt weather fluctuations and shifts in MGO behavior.

The rest of this paper is organized as follows. Section II elaborates on the modeling of MMG operating block. Then, the modeling of stochastic dynamics block is presented in Section III. Case studies are reported in Section IV. Conclusions are drawn in Section V.

II. MODELING OF MMG OPERATING BLOCK

As illustrated in Fig. 1, the proposed SEMM involves a typical smart MMG system with RES generation and multi-stakeholders. Specifically, the proposed SEMM comprises an MMG operating block and a stochastic dynamics block for the self-organizing perception of variations in the operating cost. The input of the MMG operating block includes the trading information from each MGO. Through a cooperative relationship-oriented structure, an adjacency information matrix and a state information matrix are established to characterize the operating costs of MGOs. Additionally, by considering variations in the operating cost as state transitions, the order parameters are introduced to extract statistical and probabilistic features of state transitions. These order parameters serve as inputs to the stochastic dynamics block, which mathematically characterizes state transitions as a probability-driven SDE. Specific differential terms extract state transitions caused by uncertainties while accounting for the self-organizing emergence of new states after these transitions occur. Solving the SDE with the finite difference method (FDM) yields corrected states, which are then output for MGO to optimize their energy management. In this section, we present a comprehensive description of the MMG operating block, followed by an introduction to the stochastic dynamics block in the Section III.

A. Single MG Model

The research in this paper is based on an MMG system connected to the main grid, consisting of I MGs and indexed by i . Note that there may not be a direct connection between each MG, and energy transaction is facilitated by the upper-level main grid. Moreover, we consider a discrete-time model, assuming the range is divided into K equal operation periods and indexed by k . The controllable objects at a single MG include RES, gas turbine (GT), battery energy storage system (BESS), and ET.

1) RES

A single MG is considered as an entity with RES, specifically photovoltaic (PV) and wind turbine (WT). The physical attributes of these sources are described as:

$$P_{i,k}^{\text{PV}} = \frac{H_{i,k}}{H_{i,\text{std}}} P_{i,r}^{\text{PV}} \quad (1)$$

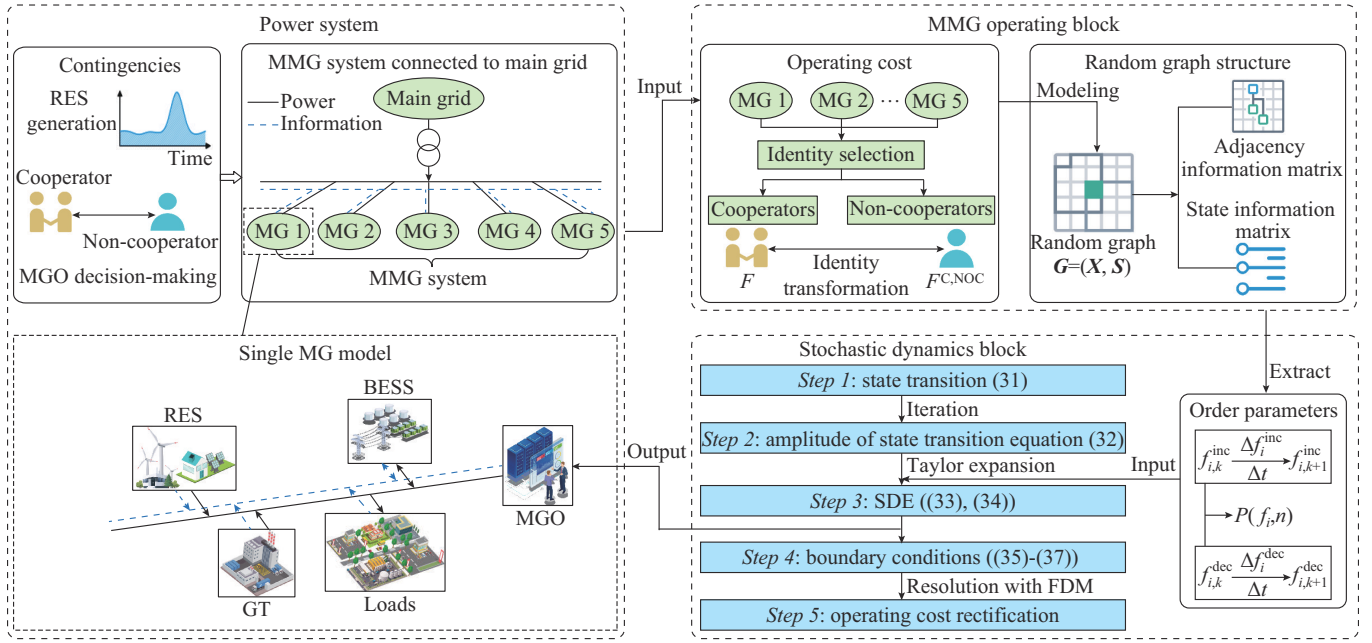


Fig. 1. Overall scheme of proposed SEMM.

$$P_{i,k}^{\text{WT}} = \begin{cases} P_{i,r}^{\text{WT}} & v_{i,r} < v_{i,k} < v_{i,out} \\ P_{i,r}^{\text{WT}} \frac{v_{i,k} - v_{i,in}}{v_{i,r} - v_{i,in}} & v_{i,in} \leq v_{i,k} \leq v_{i,r} \\ 0 & v_{i,k} < v_{i,in}, v_{i,k} > v_{i,out} \end{cases} \quad (2)$$

s.t.

$$\begin{cases} 0 \leq P_{i,k}^{\text{PV}} \leq P_{i,max}^{\text{PV}} \\ 0 \leq P_{i,k}^{\text{WT}} \leq P_{i,max}^{\text{WT}} \end{cases} \quad (3)$$

where $P_{i,k}^{\text{PV}}$ and $P_{i,k}^{\text{WT}}$ are the predicted outputs of PV and WT, respectively; $H_{i,k}$ is the predicted irradiance based on meteorological data; $H_{i,std}$ is the standard irradiance; $P_{i,r}^{\text{PV}}$ is the rated output of the PV panel; $P_{i,r}^{\text{WT}}$ is the rated output of WT; $v_{i,r}$, $v_{i,out}$, $v_{i,in}$, and $v_{i,k}$ are the rated, cut-out, cut-in, and predicted wind speeds based on meteorological data, respectively; and $P_{i,max}^{\text{PV}}$ and $P_{i,max}^{\text{WT}}$ are the upper limits for outputs of PV and WT, respectively.

2) GT

GT plays a significant role in balancing the supply and demand power of MG. The ramping constraint of GTs, indicating the difference in output power between adjacent periods, is given in (6). The mathematical model of GT is given as:

$$P_{i,k}^{\text{GT}} = V_{i,k}^{\text{gas}} C_i^{\text{gas}} \eta_i^{\text{GT}} \quad (4)$$

s.t.

$$P_{i,min}^{\text{GT}} \leq P_{i,k}^{\text{GT}} \leq P_{i,max}^{\text{GT}} \quad (5)$$

$$-U_i^{\text{down}} \Delta \tau_i^{\text{GT}} \leq P_{i,k}^{\text{GT}} - P_{i,k-1}^{\text{GT}} \leq U_i^{\text{up}} \Delta \tau_i^{\text{GT}} \quad (6)$$

where $\Delta \tau_i^{\text{GT}}$ is the adjustment time of GT; $P_{i,k}^{\text{GT}}$ is the supply power of GT; $V_{i,k}^{\text{gas}}$ is the consumption of gas; C_i^{gas} is the calorific value of gas; η_i^{GT} is the efficiency of GT; $P_{i,min}^{\text{GT}}$ and $P_{i,max}^{\text{GT}}$ are the lower and upper limits of $P_{i,k}^{\text{GT}}$, respectively; and U_i^{down} and U_i^{up} are the lower and upper limits of the ramping rate, respectively.

3) BESS

BESS is a highly efficient controllable power generation equipment. Equation (10) indicates that energy remains unchanged at the beginning and the end of a scheduling cycle. The mathematical model of the BESS is described as:

$$E_{i,k}^{\text{BESS}} = E_{i,k-1}^{\text{BESS}} + \Delta \tau_i^{\text{BESS}} \left(\eta_i^{\text{BESS, ch}} P_{i,k-1}^{\text{BESS, ch}} + \frac{P_{i,k-1}^{\text{BESS, dis}}}{\eta_i^{\text{BESS, dis}}} \right) \quad (7)$$

s.t.

$$E_{i,min}^{\text{BESS}} \leq E_{i,k}^{\text{BESS}} \leq E_{i,max}^{\text{BESS}} \quad (8)$$

$$\begin{cases} 0 \leq P_{i,k}^{\text{BESS, ch}} \leq P_{i,max}^{\text{BESS, ch}} \\ 0 \leq P_{i,k}^{\text{BESS, dis}} \leq P_{i,max}^{\text{BESS, dis}} \end{cases} \quad (9)$$

$$\sum_{k=1}^K \eta_i^{\text{BESS, ch}} P_{i,k-1}^{\text{BESS, ch}} + \sum_{k=1}^K \frac{P_{i,k-1}^{\text{BESS, dis}}}{\eta_i^{\text{BESS, dis}}} = 0 \quad (10)$$

where $E_{i,k}^{\text{BESS}}$ is the state of charge (SOC) of BESS; $P_{i,k}^{\text{BESS, ch}}$ and $P_{i,k}^{\text{BESS, dis}}$ are the charging and discharging power of BESS, respectively; $\eta_i^{\text{BESS, ch}}$ and $\eta_i^{\text{BESS, dis}}$ are the charging and discharging efficiency factors of BESS, respectively; $\Delta \tau_i^{\text{BESS}}$ is the adjustment time of BESS; $E_{i,min}^{\text{BESS}}$ and $E_{i,max}^{\text{BESS}}$ are the lower and upper limits of $E_{i,k}^{\text{BESS}}$, respectively; and $P_{i,max}^{\text{BESS, ch}}$ and $P_{i,max}^{\text{BESS, dis}}$ are the upper limits of $P_{i,k}^{\text{BESS, ch}}$ and $P_{i,k}^{\text{BESS, dis}}$, respectively.

B. Random Graph-based ET Model

To model ET patterns, we propose a dynamic identity-driven model based on the principles of random graph theory. A random graph is generated through a stochastic process, where the formation of edges between nodes follows specific probabilistic rules [24]-[26]. Specifically, as illustrated in Fig. 2, we consider a random graph with a set of nodes, where the probability of establishing an edge between any two nodes is contingent upon their respective state information. The degree of connectivity is represented by parameter

λ , which quantifies the extent of interconnections. In random graph theory, the degree is commonly employed to characterize the level of coupling between a node and the rest of the network. The mathematical representation of the random graph theory significantly simplifies the modeling complexities within intricate networks.

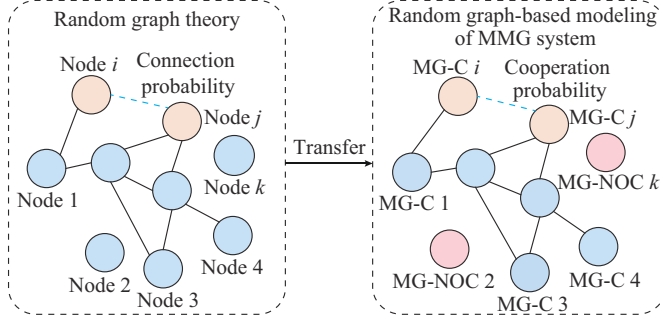


Fig. 2. Random graph-based modeling process.

Considering that the MMG system in the energy transaction operates as a point-to-point network with stochastic cooperative relationships, a generalized random graph-based modeling of MMG system is proposed to abstractly represent the virtual topology of the ET. Based on individual requirements, MGs select their own identity, which includes both cooperators and non-cooperators. The cooperator alliance refers to MGs who adopt the identity and actively participate in the transaction. In contrast, the non-cooperator alliance refers to MGs who choose not to do so. The two types of MGs are distinguished by using the abbreviations MG-C and MG-NOC in Fig. 2, respectively. Consequently, the concept of the stochastic connection is redefined as a two-dimensional and dynamic identity selection that encompasses both cooperative and non-cooperative aspects. The specific modeling steps are as follows.

The random graph of the MMG system is expressed as $\mathbf{G}=(\mathbf{X},\mathbf{S})$, where $\mathbf{X}\in\mathbf{R}^{I\times I}$ is the adjacency information matrix, which characterizes the stochastic cooperation relationships; and $\mathbf{S}\in\mathbf{R}^{I\times 14}$ is the state information matrix, which collects the meteorological and scheduling information.

1) Adjacency Information Matrix

Given the virtual nature of adjacency, this study employs random cooperative information as a representation of the adjacency information matrix \mathbf{X}_k , which is the adjacency information matrix of \mathbf{X} at the sampling time k .

$$\mathbf{X}_k=[x_{1,k},x_{2,k},\dots,x_{N,k}]^T \quad (11)$$

where $x_{i,k}\in\{0,1\}$ is the probability of MG i becoming a cooperator.

To address the limitation of disregarding the cooperative resource surplus in the model proposed in [5]-[7], we introduce the average degree λ_k to quantitatively measure the level of the cooperation readiness among MGs. λ_k is defined as:

$$\lambda_k=\langle\mathbf{G}_k\rangle=(I-1)\bar{x}_k=\frac{I-1}{I}\sum_{i=1}^I x_{i,k} \quad (12)$$

where $\langle\cdot\rangle$ is the degree of the graph; \mathbf{G}_k is the random graph of the MMG system at the sampling time k ; and \bar{x}_k is the average value of $x_{i,k}$.

2) State Information Matrix

The state information matrix \mathbf{S} , which encompasses meteorological and scheduling data of MGs, such as operating costs, control variables, equipment parameters, and meteorological data, is described as:

$$\mathbf{S}_{i,k}=[F_{i,k}^{C,\text{NOC}},\boldsymbol{\Omega}_{i,k},\mathbf{D}_{i,k}^{\text{WT}},\mathbf{D}_{i,k}^{\text{PV}}] \quad (13)$$

$$\boldsymbol{\Omega}_{i,k}=[P_{i,k}^{\text{GT}},P_{i,k}^{\text{BESS, ch}},P_{i,k}^{\text{BESS, dis}},P_{i,k}^{\text{ET}}] \quad (14)$$

$$\mathbf{D}_{i,k}^{\text{WT}}=[P_{i,r}^{\text{WT}},v_{i,r},v_{i,\text{out}},v_{i,\text{in}},v_{i,k}] \quad (15)$$

$$\mathbf{D}_{i,k}^{\text{PV}}=[H_{i,\text{std}},P_{i,\text{max}}^{\text{PV}},H_{i,k}] \quad (16)$$

where $\boldsymbol{\Omega}_{i,k}$ is the strategy information vector, which includes controllable variables of MG, incorporating the adjustment time of GT, BESS, and ET; $P_{i,k}^{\text{ET}}$ is the trading power, where $P_{i,k}^{\text{ET}}=0$ means MG i is a non-cooperator; $F_{i,k}^{C,\text{NOC}}$ is the operating cost, which is elaborated in Section II-C; and $\mathbf{D}_{i,k}^{\text{WT}}$ and $\mathbf{D}_{i,k}^{\text{PV}}$ are the matrices of equipment parameters and day-ahead meteorological data for PV and WT, respectively.

C. Operating Cost of MGs

To represent the operating cost of cooperator and non-cooperator alliances, we propose a mechanism based on a novel public goods game model [27]-[29]. In this mechanism, the interactive energy of cooperators is accumulated as individual contributions, allowing cooperators to obtain certain subsidies for participating in the proposed SEMM. Besides, identity transformation incurs additional costs. This mechanism promotes a virtuous cycle among cooperators. Note that only the prices from the buyer and seller are allowed to be transmitted within the cooperator alliance to ensure privacy and minimize information transmission.

1) Operating Cost of Cooperator Alliance

Mathematically, the operating cost based on multi-interests of a cooperator alliance F_i^C is constructed as:

$$F_i^C=\sum_{k=1}^K(C_{i,k}^{\text{GT}}+C_{i,k}^{\text{BESS}}+C_{i,k}^{\text{MAIN}}+C_{i,k}^{\text{ET}}-T_{i,k}^{\text{ET}}+C_{i,k}^{\text{NOC,C}}) \quad (17)$$

where $C_{i,k}^{\text{GT}}$ and $C_{i,k}^{\text{BESS}}$ are the operating costs of GT and BESS, respectively; $C_{i,k}^{\text{MAIN}}$ and $C_{i,k}^{\text{ET}}$ are the costs of interactive power with the main grid and other cooperators, respectively; $T_{i,k}^{\text{ET}}$ is the subsidy designed to incentivize cooperators to accumulate their contributions; and $C_{i,k}^{\text{NOC,C}}$ is the administrative cost of identity transformation.

$$C_{i,k}^{\text{GT}}=P_{i,k}^{\text{GT}}c_i^{\text{GT}} \quad (18)$$

$$C_{i,k}^{\text{BESS}}=P_{i,k}^{\text{BESS, ch}}c_i^{\text{BESS, ch}}+P_{i,k}^{\text{BESS, dis}}c_i^{\text{BESS, dis}} \quad (19)$$

$$C_{i,k}^{\text{MAIN}}=(P_{i,k}^{\text{load}}-P_{i,k}^{\text{buy}}+P_{i,k}^{\text{sell}})c_{i,k}^{\text{MAIN}} \quad (20)$$

$$C_{i,k}^{\text{ET}}=P_{i,k}^{\text{buy}}c_{i,k}^{\text{buy}}-P_{i,k}^{\text{sell}}c_{i,k}^{\text{sell}}+P_{i,k}^{\text{ET}}c_{i,k}^{\text{tra}} \quad (21)$$

$$T_{i,k}^{\text{ET}}=\frac{K}{I}\sum_{l=1}^I\varphi_{i,l}S_{i,l}P_{i,k}^{\text{ET}} \quad (22)$$

$$C_{i,k}^{\text{NOC,C}}=(s_{i,k-1}+s_{i,k})c_{i,k}^{\text{NOC,C}} \quad (23)$$

$$\begin{cases} c_i^{\text{BESS, ch}}=\alpha_i\frac{E_{i,k}^{\text{BESS}}}{E_i^{\text{total}}}+\beta_i \\ c_i^{\text{BESS, dis}}=-\alpha_i\frac{E_{i,k}^{\text{BESS}}}{E_i^{\text{total}}}+\gamma_i \end{cases} \quad (24)$$

$$\varphi_{i,k} = \varphi_{i,k-1} + \log_{\omega} \left(\frac{\lambda_{k-1}}{\lambda_k} \right) \quad (25)$$

$$P_{i,k}^{\text{ET}} = P_{i,k}^{\text{sell}} + P_{i,k}^{\text{buy}} \quad (26)$$

where c_i^{GT} is the cost of GT; $c_i^{\text{BESS, ch}}$ and $c_i^{\text{BESS, dis}}$ are the charging and discharging costs of the BESS, respectively, which are designed as a linear dynamic calculation to prevent overuse from damaging the BESS; α_i , β_i , and γ_i are the linear coefficients, which are set informed by [24]; E_i^{total} is the total capacity of BESS; $\varphi_{i,k}$ is the synergistic factor that characterizes the abundance level of heterogeneous resources of the MMG system; ω is the fixed coefficient that characterizes the fluctuation scale of the synergy factor; $P_{i,k}^{\text{buy}}$ and $P_{i,k}^{\text{sell}}$ are the purchased and bidding power, respectively; $c_{i,k}^{\text{buy}}$ and $c_{i,k}^{\text{sell}}$ are the final purchased and sell prices, respectively, which are two fixed values; κ is the fixed price coefficient, which is used for the profit reduction process of cooperators; and $c^{\text{NOC,C}}$ is the administrative cost if MG i is a non-cooperator during period $k-1$.

Herein, playing a role as cooperator alliance refers to participating in ET. Furthermore, the unit interactive power needs to pay the transmission cost c^{tra} to the main grid. We establish a priority for energy transmission between MGs over procurement from the main grid. The incentive for market enthusiasm comes from $T_{i,k}^{\text{ET}}$, that is to say, participating in the cooperator alliance can make a profit. In addition, the profit is a dynamic indicator determined by the market demand, which is defined in (22) and (25). When MG i is a cooperator, $s_{i,k}=1$; and when MG i is a non-cooperator, $s_{i,k}=0$.

2) Operating Cost of Non-cooperator Alliance

For non-cooperator alliances, although they do not participate in the state transaction, they can also receive some subsidies for playing a backup role. Mathematically, the operating cost of a non-cooperator alliance F_i^{NOC} is constructed as :

$$F_i^{\text{NOC}} = \sum_{k=1}^K (C_{i,k}^{\text{GT}} + C_{i,k}^{\text{BESS}} - T_{i,k}^{\text{NOC}} + C_{i,k}^{\text{C,NOC}}) \quad (27)$$

where $T_{i,k}^{\text{NOC}}$ is the subsidy from all cooperators according to the rules of the public goods game; and $C_{i,k}^{\text{C,NOC}}$ is the administrative cost.

$$T_{i,k}^{\text{NOC}} = \frac{\pi}{I} \sum_{\delta=1}^{N_k^{\text{C}}} T_{\delta,k}^{\text{ET}} \quad (28)$$

$$C_{i,k}^{\text{C,NOC}} = (s_{i,k-1} + s_{i,k}) c^{\text{C,NOC}} \quad (29)$$

where δ is the index of the cooperator; N_k^{C} is the number of cooperators; and π is the fixed distribution coefficient used for profit reduction process of non-cooperators.

III. MODELING OF STOCHASTIC DYNAMICS BLOCK

A. Description of Typical First-order SDE

To bolster the autonomous capabilities of MGO in dealing with contingencies, we formulate the state transition process of MMG systems as a probability-driven stochastic dynamics block. Notably, we consider the operating cost of MGO as state and its variations as state transitions.

The first-order differential equations are often used to

characterize a dynamics problem. The typical first-order SDE is illustrated as:

$$\begin{cases} dP = \mu_1 P dt + \mu_2 \tilde{W} dt \\ \tilde{W} = W + \Delta W \end{cases} \quad (30)$$

where P is the state variable; \tilde{W} and W are the actual and ideal system states, respectively; ΔW is the state transition induced by uncertainties; and μ_1 and μ_2 are the coefficients.

B. Description of Second-order SDE

Abrupt weather fluctuations and the erratic behavior of MGOs result in dynamic changes in the trends of state transitions. That is to say, the first-order differential equations allow for the representation of state transitions, akin to ‘‘velocity’’. However, they fail to capture the dynamic trends associated with these state transitions. Therefore, we propose a novel second-order SDE that incorporates specific second-order differential terms to depict the evolving trends of state transitions, which resembles ‘‘acceleration’’. By accumulating and iteratively retaining memory of these state transition trends, these second-order terms illustrate the spontaneous emergence of new states following state transitions, thereby establishing a self-organizing mechanism. The stochastic dynamics block is described in detail as follows.

1) Mathematical Preparation

Mathematically, we divide the interval between sampling points into h smaller parts Δt , so the sampling interval is represented as $t_{k \rightarrow k+1} = h\Delta t$. As mentioned above, we set $F_i^{\text{C,NOC}}$ as the state of MG i .

2) Order Parameter

In the self-organizing mechanism, there is a parameter that describes the evolutionary trend of state transitions. We define $f_{i,k}^{\text{inc}}$ and $f_{i,k}^{\text{dec}}$ as the order parameters to characterize the increasing and decreasing trends of the state transitions of MG i . According to the mathematical modeling in Section II-C, $f_{i,k}^{\text{inc}}$ is influenced by the profits and subsidies from ET, while $f_{i,k}^{\text{dec}}$ is determined by the cost of excessive device regulation and identity transformation. Furthermore, we assume that the transition rate of $f_{i,k}^{\text{inc}}$ and $f_{i,k}^{\text{dec}}$ over $t_{k \rightarrow k+1}$ is uniform, and denote their trends as Δf_i^{inc} and Δf_i^{dec} in Δt , respectively.

3) State Transition

In the presence of distinct operational environments, the probability of an individual state transition exists. We express the probability that the amplitude of state transition of MG i in a specific interval of discrete time n equals to f_i as $P(f_i, n)$. As depicted in Fig. 3, the modeling of state transition is represented as (31), which means the probability of state transition at the current state is strongly correlated with the probability at the previous state. Besides, $P(f_i - \Delta f_i^{\text{inc}}, n-1)$ and $P(f_i + \Delta f_i^{\text{dec}}, n-1)$ incorporate uncertainties into the state transition process, and also involve iterative memory of the state from the previous state, enabling the previous state to spontaneously become the source for the state at the next state.

$$P(f_i, n) = P(f_i - \Delta f_i^{\text{inc}}, n-1) + P(f_i + \Delta f_i^{\text{dec}}, n-1) - P(f_i, n-1) \quad (31)$$

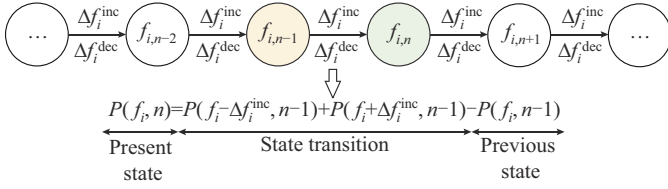


Fig. 3. Process of state transition.

4) Second-order SDE

Through iterative memorization of (31), the probability that the amplitude of state transition equals f_i within $n+l$ subintervals over any interval l is derived as:

$$P(f_i, n+l) = \begin{cases} \sum_{a,b=0}^l \frac{(-1)^{(l-a-b)} l!}{a! b! (l-a-b)!} P(f_i - a\Delta f_i^{inc} + b\Delta f_i^{dec}, n) & l-a-b > 0 \\ 0 & l-a-b \leq 0 \end{cases} \quad (32)$$

Considering the second-order state transition as the counterpart of self-organizing in second-order SDE, we perform a Taylor series expansion on (32), retaining up to the second-order SDE. To ensure the Taylor series expansion is only performed in the vicinity of f_i and to meet the requirement of small computational memory, we set $l=2$. Therefore, the second-order SDE is represented as:

$$\frac{dP(f_i, t)}{dt} = \mu_{i,k,1} \frac{d^2 P(f_i, t)}{df_i^2} - \mu_{i,k,2} \frac{dP(f_i, t)}{df_i} - \mu_{i,k,3} \frac{d^2 P(f_i, t)}{dt^2} \quad (33)$$

$$\begin{cases} \mu_{i,k,1} = (f_{i,k}^{inc})^2 - f_{i,k}^{inc} f_{i,k}^{dec} + (f_{i,k}^{dec})^2 \\ \mu_{i,k,2} = f_{i,k}^{inc} - f_{i,k}^{dec} \\ \mu_{i,k,3} = 1 \end{cases} \quad (34)$$

where $dP(f_i, t)/df_i$ is a common transition to another level state; $d^2 P(f_i, t)/df_i^2$ is a random transition to another level state caused by random disturbances; $dP(f_i, t)/dt$ is the state transition speed; $d^2 P(f_i, t)/dt^2$ is a self-organizing process, where both common and random state transitions are accelerated and self-organizing by the current state; and $\mu_{i,k,1}$, $\mu_{i,k,2}$, and $\mu_{i,k,3}$ are the dynamic coefficients of (33).

5) Boundary Conditions

To facilitate the solving approach for differential equation, the boundary conditions for potential variations are established as follows.

We assume that the probability of state transition must rapidly decrease and become 0 for high values, which means that the limit conditions are described as:

$$P(f_i, t)|_{f_i \rightarrow \pm\infty} = 0 \quad (35)$$

Regarding the initial boundary conditions, we represent them as a delta function based on objective empirical laws, implying that $P(f_i, t)$ iterates from either 0 or 1, which is expressed as:

$$P(f_i, t)|_{t=0} = \delta(f_i - 0) = \begin{cases} 1 & f_i = 0 \\ 0 & f_i \neq 0 \end{cases} \quad (36)$$

Moreover, we must also establish a third initial condition due to varying degrees of random disturbances. They affect

the rate of state transitions of MGs, causing some to experience larger changes while others weaken. Therefore, we set a periodic initial boundary condition for the rate of state transition $\partial P(f_i, t)/\partial t$ as:

$$\left. \frac{\partial P(f_i, t)}{\partial t} \right|_{t=0} = \frac{\rho(f_i + \Delta f_i, 0+t) - \rho(f_i, 0)}{\Delta t} = \frac{1}{\Delta t} \cos \frac{2\pi f_i}{\sqrt{\mu_{i,k,1}}} \quad (37)$$

where $\rho(f_i, 0)$ is the value of f_i when $t=0$.

C. Solving Approach for Proposed SEMM

To facilitate implementation, we propose a solving approach for the proposed SEMM, as outlined in Algorithm 1. Initially, we establish two finite sets of candidate strategies: a cooperative set and a non-cooperative set, distinguished by their assigned numbers. The solving approach for the proposed SEMM splits the task into two components: information extraction and self-organizing modeling. We employ the MMG operating block for the former and the stochastic dynamics block for the latter.

Algorithm 1: solving approach for proposed SEMM

1. **Initialization:** $k=1$, adjacency information matrix X , state information matrix S , and order parameters $f_{i,k=1}^{inc}$ and $f_{i,k=1}^{dec}$
2. **for** $k=1$ to K **do**
3. **for** $i=1$ to I **do**
4. Input adjacency information matrix X_k and state information matrix S_k
5. Calculate operating cost $F_{i,k}^{C,NOC}$, average degree λ_k , synergy factor at next point $\varphi_{i,k+1}$, and dynamic coefficients $\mu_{i,k,1}$, $\mu_{i,k,2}$, and $\mu_{i,k,3}$ of (33)
6. Establish boundary conditions
7. Resolve second-order SDE with FDM
8. Download the maximum amplitude $|\rho(f_{i,k,\Delta}, k)|$
9. Extract corresponding amplitude of profit shift $f_{i,k,\Delta}$
10. Update $F_{i,k+1} = F_{i,k} + f_{i,k,\Delta}$
11. Obtain strategy set corresponding to $F_{i,k+1}$
12. Update order parameters $f_{i,k+1}^{inc}$ and $f_{i,k+1}^{dec}$
- if** corresponding strategy set is cooperative
- $x_{i,k} = |\rho(f_{i,k,\Delta}, k)|$
- else**
- $x_{i,k} = 0$
- end if**
13. **end for**
14. Update S_{k+1} and X_{k+1}
15. **end for**

Initially, we set the optimization objective to minimize the operating cost of each MG and employ the MMG operating block to perceive transaction information. The resulting trend of state transition is generated as order parameters for stochastic dynamics block, which obtains the coefficients of the second-order SDE.

By integrating (33) through (35)-(37) and selecting the amplitude of state transition corresponding to the maximum amplitude $|\rho(f_{i,k,\Delta}, k)|$ as the initial value for the subsequent iteration, we can then output results based on the correspondence between the state and the strategy sets, as indicated by the adjacency information matrix S_k . Subsequently, we update the order parameters accordingly. This process is repeated until all pending energy management tasks for MMG are completed.

Note that Algorithm 1 offers a simplified solving approach for the proposed SEMM. Our primary focus in this

paper is to develop the self-organizing model and compare its performance with other models, rather than requiring a complex solving approach. However, it is worth noting that future research will explore the integration of high-performance solving approach.

IV. CASE STUDIES

A. Setup

In this study, the case overview and parameter settings are as follows: the proposed SEMM is validated with an MMG system consisting of five MGs, as illustrated in Fig. 1. Since the MGs are not physically interconnected and interact only through the main grid, the specific physical topology information is unavailable. For the analysis and explanation purposes, simulation results of three MGs from the MMG system are presented to demonstrate the feasibility of the solving approach for the proposed SEMM. Parameters of MGs and operation are detailed in Tables I and II, respectively. Moreover, we define two strategy sets: the cooperative strategy set ranges from 1 to 500 and the non-cooperative strategy set ranges from -500 to -1 . Each controllable variable exhibits a small numerical fluctuation interval of ± 5 kW. All experiments are conducted on a server equipped with CPU R93950X, GPU RTX4090, and RAM of 32 GB.

TABLE I
PARAMETERS OF MGs

MG No.	PV power (kW)	WT power (kW)	GT power (kW)	BESS power (kWh)
1	0	1500	600	500
2	1000	0	600	500
3	800	1500	600	500
4	800	1000	0	300
5	600	1500	500	500

TABLE II
PARAMETERS OF OPERATION

Parameter	Value	Parameter	Value
$P_{i,r}^{PV}$ (kW)	350	$\eta^{BESS, ch}, \eta^{BESS, dis}$	0.97, 0.95
$P_{i,r}^{WT}$ (kW)	800	α, β, γ (¥)	1.5, 6.1, 4.2
$P_{max}^{BESS, ch}, P_{max}^{BESS, dis}$ (kW)	150, 150	C^{buy}, C^{sell}	0.55, 0.55, 0.55
$E_{min}^{BESS}, E_{max}^{BESS}$ (p.u.)	0.1, 0.9	C^{MAIN} (¥/kWh)	0.1
η^{GT}	0.3	c^{MAIN} (¥/kWh)	0.1
$c^{NOC, C}, c^{C, NOC}$ (¥)	50, 200	κ, ω, π	2, 0.5, 0.8

B. Results and Analysis of MMG Operating Block

Figure 4 displays energy management results without ET. The adjustable resources in each MG exhibit frequent adjustments and poor stability. The energy management results with ET are shown in Fig. 5. For instance, MG 1 adopts the cooperative identity for nearly 20 hours with the assistance of the mechanism. During the WT peak periods, an average of 186.92 kW is sold per sample point, while an average of 213.46 kW is purchased during the load peak periods. Moreover, the frequency of adjustments for BESS and GT are de-

creased by 10.31% and 63.86%, respectively, leading to an increase in economic profits of 41.32%.

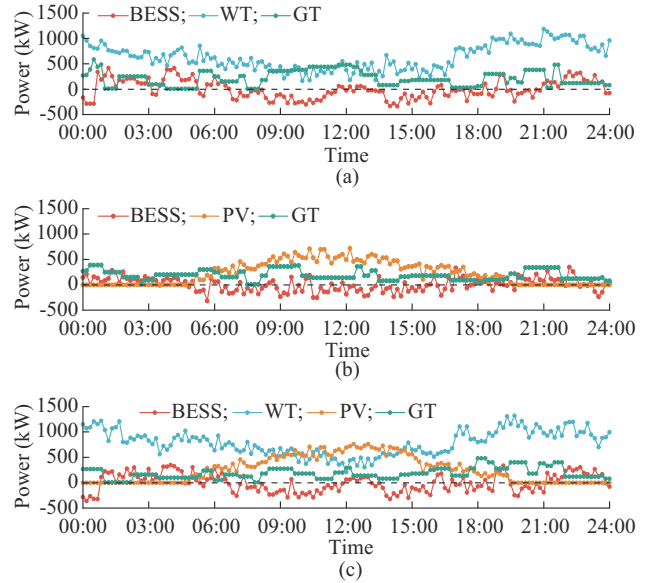


Fig. 4. Energy management results without ET. (a) MG 1. (b) MG 2. (c) MG 3.

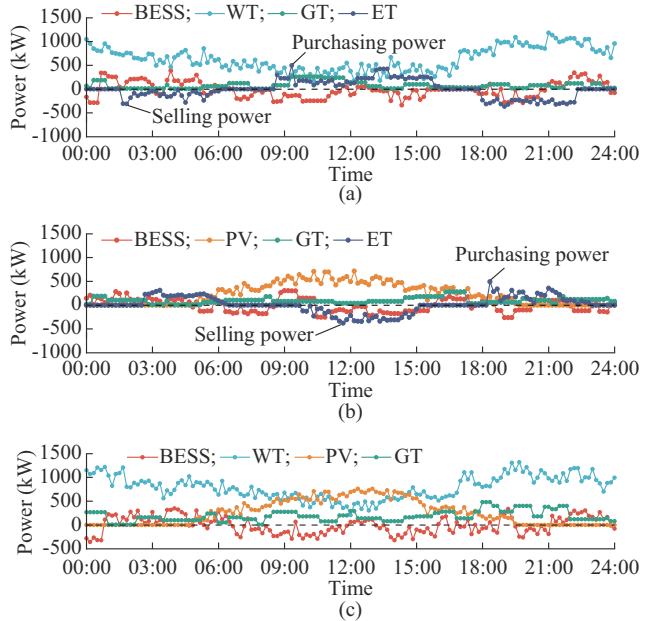


Fig. 5. Energy management results with ET. (a) MG 1 (b) MG 2 (c) MG 3.

For MG 3, however, it selects the non-cooperative identity almost all the time. The analysis indicates that both MG 1 and MG 2 have only one highly penetrative RES, and the volatility of the RES makes it difficult for them to increase profits through less self-adjustment of resources. Therefore, they would rather choose to cooperate even if they have to pay certain fees for transmission and platform management. MG 3 possesses a diverse set of energy sources, which results in a relatively smaller impact on profits. Therefore, MG 3 chooses the non-cooperative identity for a prolonged period. The results demonstrate that a flexible interaction framework based on dynamic identities is a more rational

and effective approach for MMG systems.

C. Comparison of First-order and Second-order SDEs

To visually demonstrate the equation performance of the proposed SEMM, the comparison of decision-making process is depicted in Fig. 6, we compare the distribution of scheme selection across three stages in first-order and second-order SDEs. Figure 6 depicts a multi-factor grouped boxplot. The boxes represent the range of scheme numbers occupying from 25% to 75% of the total count. The whiskers in the box plot depict the entire range of values. The “points + curves” on the right side of the boxes illustrate the distribution of scheme numbers, with the “points” representing the optimal scheme number and outlier numbers. Additionally, the mean of each distribution group is annotated on Fig. 6.

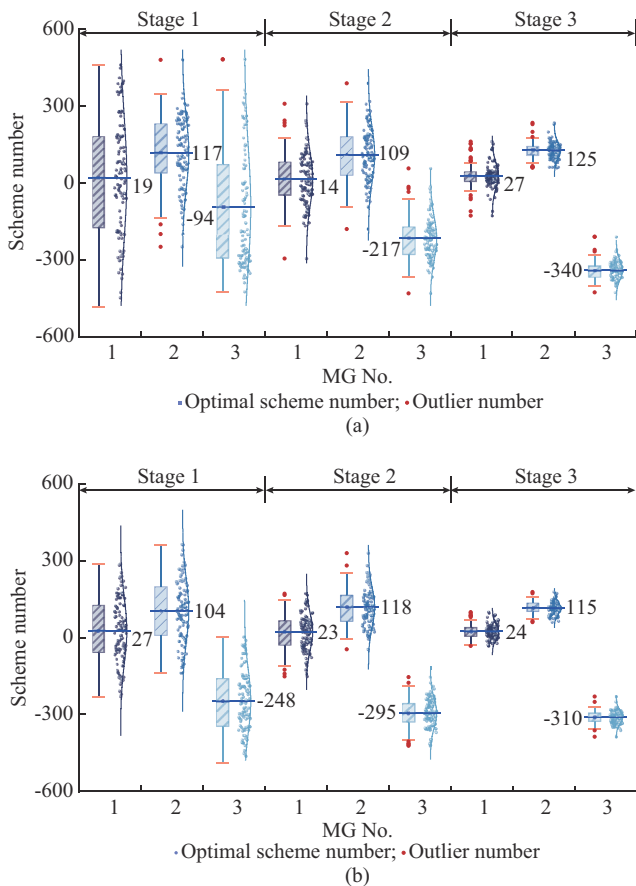


Fig. 6. Comparison of decision-making process. (a) First-order SDE. (b) Second-order SDE.

The second-order SDE outperforms the first-order SDE. In the initial stage 1, the second-order SDE sets the initial collaborative factor to be 0.8, which encourages the SDE to explore more feasible schemes and accumulate some preliminary “memory”. Thus, the distribution of the schemes fluctuates significantly during the phase of iterative experimentation and refinement, but the second-order SDE still performs better.

Subsequently, from the mid-term stage 2 to the later stage 3, as the synergistic factor dynamically decreases, based on

accumulated “memory”, the second-order SDE can perceive information and obtain the optimal scheme by itself. Therefore, it converges faster and more stable. Specifically, for MG 2, the variance of the scheme number across the three stages for the second-order SDE is 35.95, lower than 2.67 for the first-order SDE. Moreover, the frequency of outlier occurrence is 18.34% lower than that of the first-order SDE.

D. Analysis of Addressing Contingencies

The subsequent analysis pertains to the performance of the proposed SEMM in addressing contingencies. As mentioned in Section I, contingencies in MMG system are typically characterized by the randomness of the individual management behaviors and the volatility of RES. Therefore, we consider the chance of increase in WT output and the random addition of multiple new entities to the MMG system as small and large disturbances, respectively. Two novel data-driven models, DR model [11]-[14] and POMDP model [16]-[18], are selected for comparison to analyze the spontaneous capabilities after contingencies occur.

1) Benchmark Analysis

We conduct a benchmark of the performance of the three models under normal conditions without any contingency. For the DR model, the real prediction error is used as the uncertainty set, and the algorithm parameters are set based on [30]. In the case of POMDP model, we utilize actual data from the first 20 days of a particular month as the training set for the agent, and the last 10 days as the test set. During the training process, the learning rate and the discount factor are set as 0.01 and 0.9, respectively [18].

The economic performance of the three models under the benchmark condition is similar, as demonstrated in Fig. 7(a). However, during the majority of periods, DR and POMDP models exhibit slightly better economic performance than the proposed SEMM. A statistical test is conducted with a significance level of 0.05 to confirm this finding. The p-value is greater than 0.05, indicating that there is no statistically significant difference in the economic performance among the three models. In the absence of random disturbances, the proposed SEMM does not appear to be the optimal choice when compared to the advanced modeling models.

2) Contingency 1: Accidental WT Fluctuation at 06:00

The accidental WT fluctuation has a relatively significant impact on the energy management of MG systems. However, it does not substantially disrupt the stable operating rules of the overall system. Therefore, we introduce it as a mild disturbance at 06:00 and observe the performance of self-governing for three models after the contingency.

Taking MG 1 as an example and adopting the cooperative identity, Fig. 8 illustrates an average increase in WT output of 31.62% at 06:00. The analysis reveals that DR model addresses this contingency by utilizing the maximum capacity of the BESS to store energy. However, in numerical terms, DR model decreases the overall revenue by 4.59% compared with the benchmark. Therefore, while DR model shows effectiveness in managing WT contingencies, its impact on the economic performance of the system requires careful evaluation.

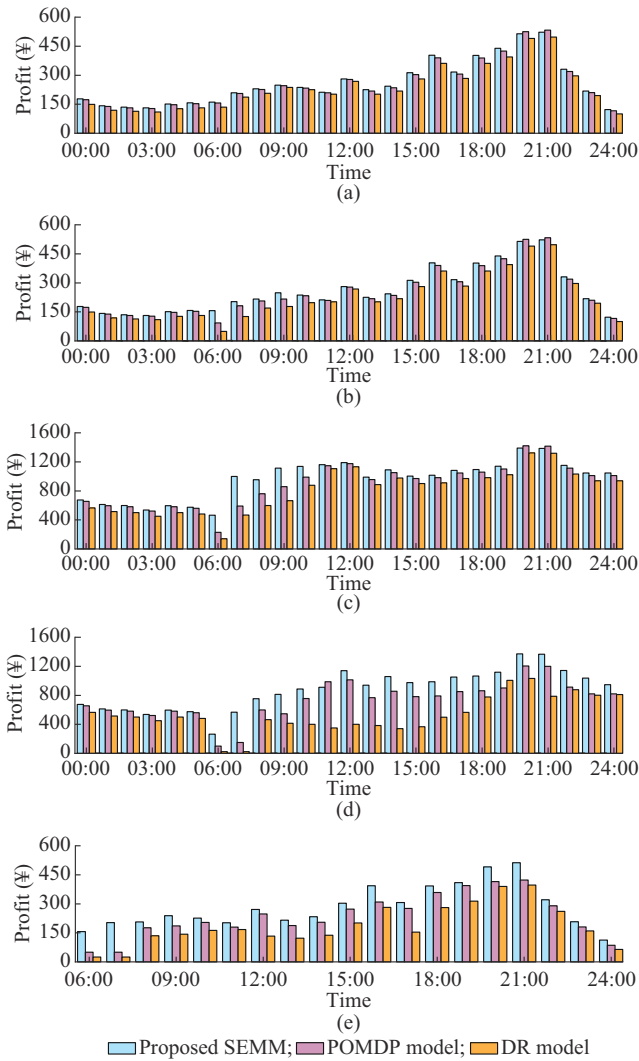


Fig. 7. Economic performance of three models. (a) MG 1 in benchmark. (b) MG 1 in contingency 1. (c) MG 3 in contingency 1. (d) MG 3 in contingency 2. (e) MG 6 in contingency 2.

However, the proposed SEMM and POMDP model demonstrate superior economic performance due to their adaptive use of the cooperative identity. Specifically, the proposed SEMM achieves a 13.52% increase and the POMDP model achieves a 10.18% increase in revenue compared with the DR model. Furthermore, the proposed SEMM shows a 13.73% increase in energy transactions compared to POMDP model. This analysis suggests that leveraging the rules of the free market in a self-organizing way during mild disturbances could enhance the economic performance.

Similarly, we analyze the behavior of MG 3 within the non-cooperator alliance. As shown in Fig. 9, the DR model exhibits consistent responses to the WT fluctuation as previously described. Due to the fixed identity of MG 3 during the training set period, the POMDP model initially maintains its non-cooperative identity. However, it struggles with equipment stability, requiring adjustments more frequently than the proposed SEMM by 28.85%. The dynamic adjustment of the proposed SEMM of the cooperative factor prompts MG 3 to transition into a cooperator role during this period, ac-

tively engaging in ET. Notably, between 08:00 and 24:00, MG 3 autonomously reverts to a non-cooperative identity, prioritizing self-sufficiency.

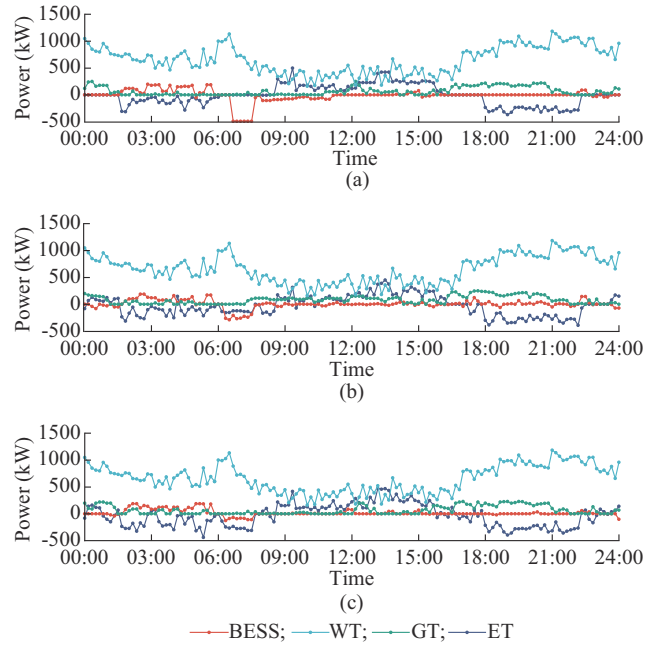


Fig. 8. Comparison of energy management results for MG 1 in contingency 1. (a) DR model. (b) POMDP model. (c) Proposed SEMM.

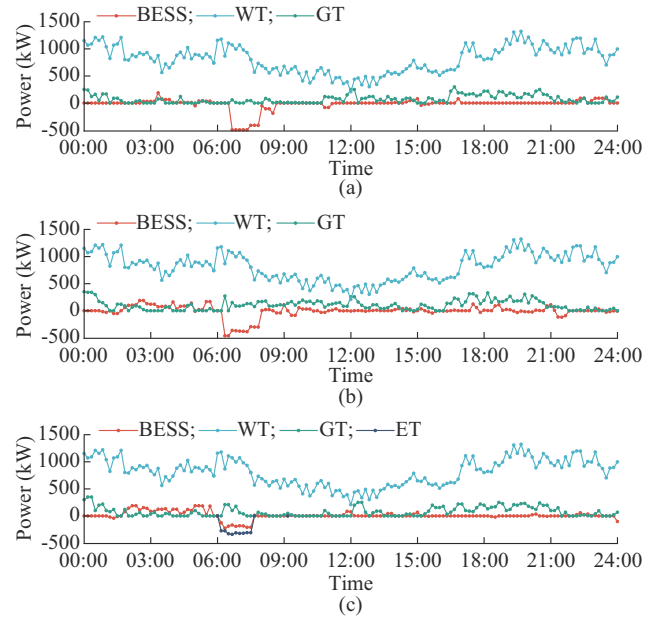


Fig. 9. Comparison of energy management results for MG 3 in contingency 1. (a) DR model. (b) POMDP model. (c) Proposed SEMM.

3) Contingency 2: Expansion of MMG System at 06:00

To validate the self-organizing capability under large-scale disturbances, we introduce three new MGs into the original MMG system at 06:00. These MGs share identical parameters with MGs 1-3 but lack historical data. For cooperators, the entry of additional MGs into the MMG system reinforces their cooperative identity, which requires no further discussion.

In the case of MG 3, as depicted in Figs. 7(d) and 10, the proposed SEMM demonstrates superior economic performance compared with DR and POMDP models, although it experiences a restructuring of the revenue structure at 06:00. A detailed examination reveals that they experience algorithm shutdown for approximately 1.2 and 2.0 hours, respectively, before resuming operation. The shutdown incapacitates them from making decisions, resulting in an average economic downturn of 171.8 and 282.9 ¥/hour, respectively. In contrast, the proposed SEMM continues to cooperate with others during the disturbance, with a slight impact on the economic performance.

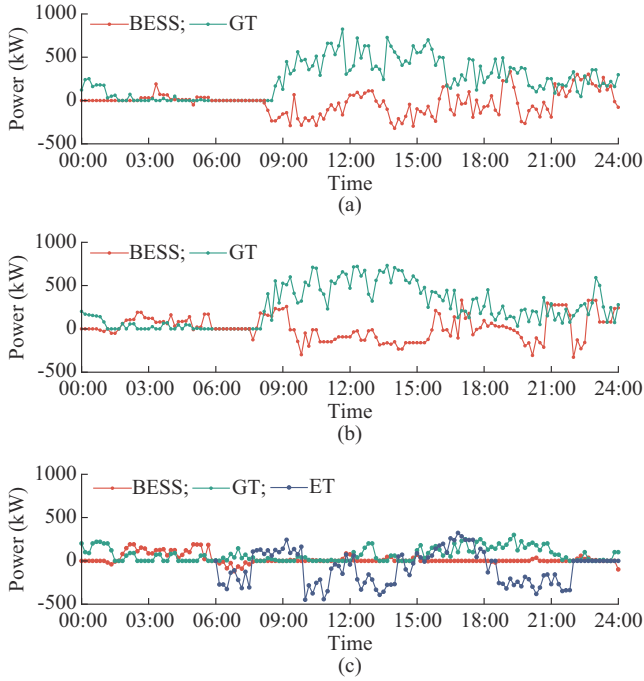


Fig. 10. Comparison of energy management results for MG 3 in contingency 2. (a) DR model. (b) POMDP model. (c) Proposed SEMM.

After the restart, MG 3 in the proposed SEMM maintains the cooperative identity for 15.3 hours to avoid a higher device adjustment frequency. However, the DR and POMDP models maintain the non-cooperative identity, resulting in a device adjustment frequency, which is 31.17% and 21.02% higher than that of the proposed SEMM, respectively. The economic performance also declines by 39.33% and 16.26%, respectively. These results highlight the instability of DR and POMDP models when faced with randomness and unfamiliar historical data of new entities.

However, as shown in Fig. 11, the economic performance of the proposed SEMM for MG 6 is slightly inferior to that for MG 1 with similar parameters due to the unfamiliarity of the new entity. Specifically, the device adjustment frequency is 14.48% higher than that of MG 1, resulting in a 3.76% reduction in profit. This indicates that the proposed SEMM adopts a conservative management approach when dealing with a new entity for the first time, which could be an area for improvement in the future research.

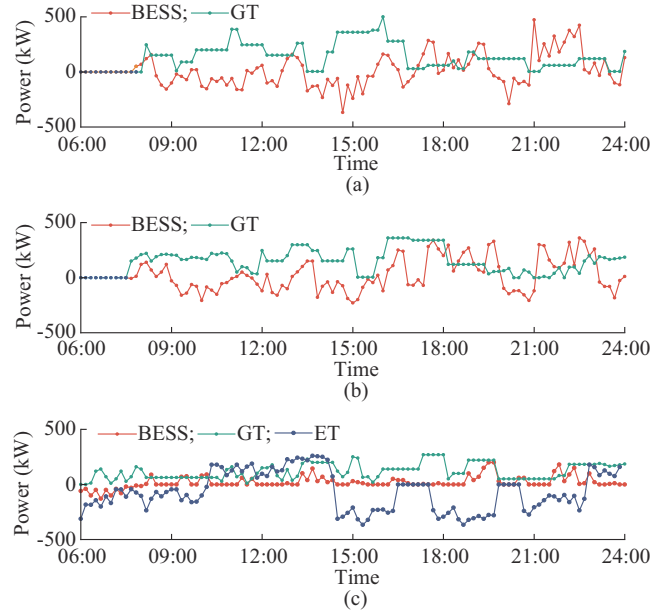


Fig. 11. Comparison of energy management results for MG 6 in contingency 2. (a) DR model. (b) POMDP model. (c) Proposed SEMM.

V. CONCLUSION

This study proposes an SEMM to enhance the economic performance of MGOs in contingencies. The proposed SEMM incorporates an identity-based MMG operating block and stochastic dynamics block that applies second-order SDE to accurately characterize the self-organizing evolution of the operating cost incurred by contingencies. Specifically, the MMG operating block relies on two random graph-driven information matrices and introduces order parameters to extract probabilistic properties of variations in the operating cost. These order parameters are then input into the stochastic dynamics block with SDEs resolved by FDM. The main conclusions can be given as follows.

1) The identity-based cooperation mechanism within the MMG operating block effectively reduces the need for frequent equipment adjustments, thereby improving cost-effectiveness.

2) The second-order SDE demonstrates enhanced stability and faster convergence compared with the first-order SDE.

3) In stable scenarios, the proposed SEMM performs comparably to state-of-the-art data-driven models such as DR and POMDP models. However, when faced with contingencies accompanied by sparse historical data, the proposed SEMM exhibits remarkable autonomous adjustment capabilities.

Future research directions include the development of enhanced stochastic dynamics approaches integrating high-performance solution algorithms to effectively manage contingencies arising from fragmented and aggregated resource integration.

REFERENCES

- [1] Y. Li and F. Nejabatkhah, "Overview of control, integration and energy management of microgrids," *Journal of Modern Power Systems and Clean Energy*, vol. 2, no. 3, pp. 212-222, Aug. 2014.

- [2] B. Zhou, J. Zou, C. Y. Chung *et al.*, "Multi-microgrid energy management systems: architecture, communication, and scheduling strategies," *Journal of Modern Power Systems and Clean Energy*, vol. 9, no. 3, pp. 463-476, May 2021.
- [3] P. Kou, D. Liang, and L. Gao, "Distributed EMPC of multiple microgrids for coordinated stochastic energy management," *Applied Energy*, vol. 185, pp. 939-952, Jan. 2017.
- [4] S. Li, D. Cao, W. Hu *et al.*, "Multi-energy management of interconnected multi-microgrid system using multi-agent deep reinforcement learning," *Journal of Modern Power Systems and Clean Energy*, vol. 11, no. 5, pp. 1606-1617, Sept. 2023.
- [5] S. Park, J. Lee, S. Bae *et al.*, "Contribution-based energy-trading mechanism in microgrids for future smart grid: a game theoretic approach," *IEEE Transactions on Industrial Electronics*, vol. 63, no. 7, pp. 4255-4265, Jul. 2016.
- [6] A. M. Jadhav, N. R. Patne, and J. M. Guerrero, "A novel approach to neighborhood fair energy trading in a distribution network of multiple microgrid clusters," *IEEE Transactions on Industrial Electronics*, vol. 66, no. 2, pp. 1520-1531, Feb. 2019.
- [7] M. Yan, M. Shahidehpour, A. Paaso *et al.*, "Distribution network-constrained optimization of peer-to-peer transactive energy trading among multi-microgrids," *IEEE Transactions on Smart Grid*, vol. 12, no. 2, pp. 1033-1047, Mar. 2021.
- [8] K. Antoniadou-Plytaria, D. Steen, L. A. Tuan *et al.*, "Scenario-based stochastic optimization for energy and flexibility dispatch of a microgrid," *IEEE Transactions on Smart Grid*, vol. 13, no. 5, pp. 3328-3341, Sept. 2022.
- [9] J. Lee, S. Lee, and K. Lee, "Multistage stochastic optimization for microgrid operation under islanding uncertainty," *IEEE Transactions on Smart Grid*, vol. 12, no. 1, pp. 56-66, Jan. 2021.
- [10] B. Chen, J. Wang, X. Lu *et al.*, "Networked microgrids for grid resilience, robustness, and efficiency: a review," *IEEE Transactions on Smart Grid*, vol. 12, no. 1, pp. 18-32, Jan. 2021.
- [11] Y. Tang, Q. Zhai, and J. Zhao, "Multi-stage robust scheduling for community microgrid with energy storage," *Journal of Modern Power Systems and Clean Energy*, vol. 11, no. 6, pp. 1923-1934, Nov. 2023.
- [12] X. Shi, Y. Xu, Q. Guo *et al.*, "Day-ahead distributionally robust optimization-based scheduling for distribution systems with electric vehicles," *IEEE Transactions on Smart Grid*, vol. 14, no. 4, pp. 2837-2850, Jul. 2023.
- [13] Y. Liu, X. Chen, L. Wu *et al.*, "Distributionally robust economic dispatch using IDM for integrated electricity-heat-gas microgrid considering wind power," *CSEE Journal of Power and Energy Systems*, vol. 9, no. 3, pp. 1182-1192, May 2023.
- [14] S. Babaei, R. Jiang, and C. Zhao, "Distributionally robust distribution network configuration under random contingency," *IEEE Transactions on Power Systems*, vol. 35, no. 5, pp. 3332-3341, Sept. 2020.
- [15] L. M. Maillart, "Maintenance policies for systems with condition monitoring and obvious failures," *IIE Transactions*, vol. 38, no. 6, pp. 463-475, Jul. 2006.
- [16] J. Qi, L. Lei, K. Zheng *et al.*, "Optimal scheduling in IoT-driven smart isolated microgrids based on deep reinforcement learning," *IEEE Internet Things Journal*, vol. 10, no. 18, pp. 16284-16299, Sept. 2023.
- [17] D. Qiu, Y. Wang, T. Zhang *et al.*, "Hierarchical multi-agent reinforcement learning for repair crews dispatch control towards multi-energy microgrid resilience," *Applied Energy*, vol. 336, p. 120826, Apr. 2023.
- [18] Y. Gu and X. Huang, "A reactive power optimization partially observable Markov decision process with data uncertainty using multi-agent actor-attention-critic algorithm," *International Journal of Electrical Power & Energy Systems*, vol. 147, p. 108848, May 2023.
- [19] Y. Gu and X. Huang, "Demand response-based autonomous voltage control for transmission and active distribution networks using modified partially observed Markov decision process model," *IET Generation, Transmission & Distribution*, vol. 17, no. 23, pp. 5155-5170, Dec. 2023.
- [20] J. P. Gleeson, "Binary-state dynamics on complex networks: pair approximation and beyond," *Physical Review X*, vol. 3, no. 2, pp. 21004-21016, Apr. 2013.
- [21] D. Zhukov, T. Khvatova, C. Millar *et al.*, "Modelling the stochastic dynamic of transitions between states in social systems incorporating self-organization and memory," *Technological Forecasting and Social Change*, vol. 158, pp. 120134-120142, Sept. 2020.
- [22] D. Zhukov, T. Khvatova, C. Millar *et al.*, "Beyond big data-new techniques for forecasting elections using stochastic models with self-organisation and memory," *Technological Forecasting and Social Change*, vol. 175, pp. 121425-121435, Feb. 2022.
- [23] Z. Chen, J. Chen, and L. Wan, "Self-organized cooperative regulation strategy for multi-microgrid-distribution network based on stochastic evolutionary dynamics," *Automation in Electric Power Systems*, vol. 47, no. 2, pp. 24-33, Jan. 2023.
- [24] Z. Zhao, J. Guo, X. Luo *et al.*, "Distributed robust model predictive control-based energy management strategy for islanded multi-microgrids considering uncertainty," *IEEE Transactions on Smart Grid*, vol. 13, no. 3, pp. 2107-2120, May 2022.
- [25] M. E. Zhukovskii and A. M. Raigorodskii, "Random graphs: models and asymptotic characteristics," *Russian Mathematical Surveys*, vol. 70, no. 1, pp. 33-81, Feb. 2015.
- [26] B. K. Fosdick, D. B. Larremore, J. Nishimura *et al.*, "Configuring random graph models with fixed degree sequences," *SIAM Review*, vol. 60, no. 2, pp. 315-355, Jan. 2018.
- [27] J. He, J. Wang, F. Yu *et al.*, "The persistence and transition of multiple public goods games resolves the social dilemma," *Applied Mathematics and Computation*, vol. 418, p. 126858, Apr. 2022.
- [28] Z. Rong and Z. Wu, "Effect of the degree correlation in public goods game on scale-free networks," *EPL (Europhysics Letters)*, vol. 87, no. 3, pp. 30001-30016, Aug. 2009.
- [29] A. Szolnoki and M. Perc, "Reward and cooperation in the spatial public goods game," *EPL (Europhysics Letters)*, vol. 92, no. 3, pp. 38003-38005, Nov. 2010.
- [30] Y. Gu, X. Huang, and Z. Chen, "A data-driven multi-stage stochastic robust optimization model for dynamic optimal power flow problem," *International Journal of Electrical Power & Energy Systems*, vol. 148, pp. 108955-108970, Jun. 2023.

Jiachen Chen received the B.S. degree from Chien-Shiung Wu College, Southeast University, Nanjing, China, in 2022. He is currently pursuing the Ph.D. degree in electrical engineering at Southeast University. His research interest includes efficient operation of multi-microgrid systems.

Zhong Chen received the B.S., M.S., and Ph.D. degrees from the School of Electrical Engineering, Southeast University, Nanjing, China, in 1999, 2002, and 2006, respectively. He is currently a Full Professor with Southeast University and was a Senior Visiting Scholar at the University of Bath, Bath, UK and Queen's University Belfast, Belfast, UK, from 2006 to 2007. He now serves as the Vice-chairman of the IEEE PES Power Grid Stability Control Technology Subcommittee. His research interests include electric vehicle, renewable energy, and integrated power system operation and control.

Qiang Xing received the Ph.D. degree in electrical engineering from Southeast University, Nanjing, China, in 2022. From 2021 to 2022, he was a joint Ph.D. student with Nanyang Technological University, Singapore. He is currently a Lecturer at Nanjing University of Posts and Telecommunications, Nanjing, China. His research interests include integration of electric vehicle and transportation-electrification network.